Nat. Hazards Earth Syst. Sci. Discuss., 3, 497–533, 2015
www.nat-hazards-earth-syst-sci-discuss.net/3/497/2015/
doi:10.5194/nhessd-3-497-2015

Natural Hazards and Earth System Sciences
Discussions
Open Access

Assessment of impact of mass movements on the upper Tayyah valley's bridge along Shear escarpment highway, Asir region (Saudi Arabia) using remote sensing data and field investigation

A. M. Youssef[1,2], M. Al-Kathery[2], and B. Pradhan[3]

[1]Geology Department, Faculty of Science, Sohag University, Egypt
[2]Geological Hazards Department, Applied Geology Sector, Saudi Geological Survey, 54141, Jeddah 21514, KSA
[3]Department of Civil Engineering, Geospatial Information Science Research Center (GISRC), Faculty of Engineering, University Putra, Malaysia

Received: 30 September 2014 – Accepted: 16 December 2014 – Published: 20 January 2015

Correspondence to: B. Pradhan (biswajeet24@gmail.com)

Published by Copernicus Publications on behalf of the European Geosciences Union.

Assessment of impact of mass movements on the upper Tayyah valley's bridge

A. M. Youssef et al.

Abstract

Escarpment highways, roads and mountainous areas in Saudi Arabia are facing landslide hazards that are frequently occurring from time to time causing considerable damage to these areas. Shear escarpment highway is located in the north of the Abha city. It is the most important escarpment highway in the area, where all the light and heavy trucks and vehicle used it as the only corridor that connects the coastal areas in the western part of the Saudi Arabia with the Asir and Najran Regions. More than 10 000 heavy trucks and vehicles use this highway every day. In the upper portion of Tayyah valley of Shear escarpment highway, there are several landslide and erosion potential zones that affect the bridges between tunnel 7 and 8 along the Shear escarpment Highway. In this study, different types of landslides and erosion problems were considered to access their impacts on the upper Tayyah valley's bridge along Shear escarpment highway using remote sensing data and field investigation. These landslides and erosion problems have a negative impact on this section of the highway. Results indicate that the areas above the highway and bridge level between bridge 7 and 8 have different landslides including planar, circular, rockfall failures and debris flows. In addition, running water through the gullies cause different erosional (scour) features between and surrounding the bridge piles and culverts. A detailed landslides and erosion features map was created based on intensive field investigation (geological, geomorphological, and structural analysis), and interpretation of Landsat image 15 m and high resolution satellite image (QuickBird 0.61 m), shuttle radar topography mission (SRTM 90 m), geological and topographic maps. The landslides and erosion problems could exhibit serious problems that affect the stability of the bridge. Different mitigation and remediation strategies have been suggested to these critical sites to minimize and/or avoid these problems in the future.

NHESSD

3, 497–533, 2015

Title Page
Abstract | Introduction
Conclusions | References
Tables | Figures
◂◂ | ▸▸
◂ | ▸
Back | Close
Full Screen / Esc
Printer-friendly Version
Interactive Discussion

1 Introduction

Landslides are one of the natural hazards that cause serious economic and live losses every year all over the world. They hit mountainous areas and highways from time to time due to different triggering factors. In mountainous areas of the southern Saudi Arabia, there are lots of urban areas, highways, roads, and escarpment roads that are prone to different types of landslides (Youssef et al., 2024a). Mass wasting problems were encountered in the different parts of Saudi Arabia including rockfalls, debris flows, and sliding (planar, wedge, and circular failures) (Youssef et al., 2012). Among these landslide problems; Al-Hada debris flow in August 2012 (Youssef et al., 2013) and Al-Raith debris flow in March 2013 (Youssef et al., 2014b). These landslides are caused due to natural triggering factors such as rain storm events and anthropogenic effects (rock cuts and dumping materials along the gullies and streams).

Landslides represent a type of mass movements that happen due to a variety and combination of different processes, including falls, topples, avalanches, slides, and flows (Regmi et al., 2013a, 2013b; Shroder and Bishop, 1998). Different factors such as seismic activity, blasting, stress release, high groundwater pressures (after heavy rainfall) and climate changes, freeze-thaw, thermal cycling, chemical weathering (its rate increases with the presence of water and gasses), snowmelt, channel runoff, geological factors such as rock types and discontinuities, truck vibration, debris materials availability in streams, soil decomposition, and human activities can trigger large rock/soil blocks or even larger assemblages of rock to crash down on to the road surface below (Baum and Godt, 2010; Franklin and Senior, 1997; Kuhnel, 2004; Guzzetti et al., 2008; Iverson et al., 2011; Youssef et al., 2012). In recent years, assessment of landslide susceptibility have been attempted by several researchers using different approaches (Carrara et al., 1995; Chung and Fabbri, 1999; Dhakal et al., 2000; Fell et al., 2008; Guzzetti et al., 1999; Lan et al., 2004; Van Westen, 1994). In addition, many authors studied the debris flows, their types, and mechanisms, among them, Hungr et al. (2001); Johnson (1984); Pierson and Costa (1987); Youssef et al. (2012, 2014b).

NHESSD
3, 497–533, 2015

Due to the high density and mobility of debris flows, they represent a serious hazard, which impose serious problems for people, properties, vehicles, and infrastructure in mountainous regions. In addition different authors indicated the hazard impact of the debris flows (Hungr et al., 1987; Prochaska et al., 2008).

Materials collected in the ravines, gullies, and streams are related to different types of landslides along the sides of the networks. These slope failures can be classified into two groups; first group is depending on the geometrical and mechanical nature of the discontinuities and the conditions of the rock masses which include circular, planar, wedge, and toppling failures (Farrokhnia et al., 2010; Regmi et al., 2014; Youssef et al., 2012, 2014b). The second group is rock failure by raveling failure mechanism which cannot be analyzed using limiting equilibrium analysis. According to the advancing of the remote sensing and GIS applications, landslide susceptibility mapping become easier and well known and used in the preliminary assessment of different areas (Pourghasemi et al., 2012; Shahabi et al., 2014; Tien Bui et al., 2012; Umar et al., 2014) Landslide types such as structural control, raveling types, and debris flow need a mitigation strategies that may be required to minimize their risks which have been applied in many research areas (Frenez et al., 2004; Maerz et al., 2014; Rickenmann, 1999; Rimbock and Strobl, 2002; Youssef et al., 2012, 2014b). Using the high-resolution satellite images, historical landslides could be observed as breaks in the highly vegetated area, bare soil, or geomorphological features, such as head and side scarps, flow tracks, and soil and debris deposits below a scar (De la Ville et al., 2002; Youssef et al., 2009).

The current study deals with the evaluation, mapping, and determination of the characteristics of the different types of problems related to landslides and erosion features and their impacts on the highway section (bridge section).

This requires identification of all landslide types and erosion features along the escarpment highways section (bridge section) from tunnel 7 to tunnel 8. This zone is a landslide prone zone due to the adverse geological formation, structural features, steep slopes, drainage gullies and rills, highly dissected topography, and rainfall impacts. Therefore, it was pertinent to assess the hazards associated with the existing and potential landslides along this section of the important escarpment Highway in the Tayyah valley.

2 Study area

The Shear escarpment highway is located in the Asir region, Saudi Arabia (Fig. 1a). It represents a part of Abha Highland (which is related to Arabian shield). It descends from the top of the escarpment (highly rigged mountains) near the Abha City down to the Mahail Asir then to the coastal zone of the western Saudi Arabia (Fig. 1b). It connects the Red Sea coastal areas (western region of the Saudi Arabia) with the Asir and Najran regions. This escarpment road was one of the first roads in the area constructed through this extremely difficult mountainous terrain almost 32 years ago. It is an important escarpment highway, as it offers access to the private vehicles, light-duty trucks, and the only escarpment highway for the heavy duty trucks. The Shear escarpment highway is about 16 km long, measured from the top of the escarpment (2200 m a.s.l.) from east to the Mahail Asir city (approximately 700 m a.s.l.). The highway is characterized by the presence of about 11 tunnels and many curvatures as well as some bridges. The current study was carried out to deal with the main bridge section (with a length of 2150 m) between tunnels 7 (at elevation of 1888 m) and 8 (at elevation of 2004 m) which are located at the upper reache of Tayyah valley (Fig. 1b). The area is located on a small wadi that meets at a right angle with the main wadi of Tayyah (Fig. 1b). The small wadi that includes the study area is surrounded by high mountains with high slopes. It appears as a deep and narrow gorge. This tributary (small wadi) flows with great force in steep and narrow channels often resulting in excessive toe erosion. The area is commonly prone to landslide activities (rock falls, sliding, and debris flows) and erosion due to running water through different gullies. There are numbers of active landslides which are badly affecting the highway and bridges and are the potential sites to cause disaster in the event of a major rainfall or earthquake.

3 Methodology

In general practice, landslide hazard of an area is assessed by carrying out intensive field investigation, remote sensing data analysis, interpretation of geological and topographical data. This is usually accomplished by the analysis of several factor maps and landslide distribution of the area to classify them into various types. In the present work, assessment of landslide and erosion problems have been carried out with the help of different types of data (Fig. 2). Lithological, morphological, hydrological, and structural characteristics of the study area might have influenced the distribution of landslides and erosional features. The geological and structural data were mapped according to the Abha quadrangle geological map (GM-75, 1 : 250 000 scale). These geological and structural data were verified in the field. Different types of information were collected using standard field investigation techniques. Many structural data were measured including joint planes and minor faults. All landslides, in the study highway section from tunnel 7 to tunnel 8 in the upper portion of the Tayyah valley, were identified and mapped using remote sensing data (landsat image (ETM^+ 15 m resolution), high resolution satellite images (QuickBirds 0.61 m spatial resolution), and Shuttle Radar Topography Mission (SRTM 90 m), topographic map (scale 1 : 10 000), and verified using intensive field investigation. Besides mapping the different types of landslides, rock mass rating (RMR) for different rock zones in the study area was identified to determine the quality of these rocks and to classify the study area into zones. Different rock samples were collected from the different landslide zones in order to apply rock shear test to determine the friction angle for rock plane sliding. In addition gullies that dissect the study area were mapped and different morphometric parameters were determined using watershed modeling system (WMS8.1). Different features of landslides and erosions were mapped using rigorous field investigation and from the high resolution satellite image. Potential for planner failures was carried out using Dips 5 program (RocScience, 1999). The remote sensing based analysis, field, and laboratory studies

NHESSD
3, 497–533, 2015

were coupled together to get the comprehensive view of the different types of landslide and erosion features that impose a high impact on the study area.

4 Geomorphology, geological/structural setting and climatic characteristics

Geomorphologically, the study area is located at the upper portion of Tayyah valley. The escarpment itself is the result of erosional retreat of uplifted Precambrian rocks that were elevated concurrent with initiation of rifting in the Red Sea during the late Paleogene era. The escarpment runs in different direction such as east–west and north–south. Whereas, the study area has a curvature shape (Fig. 1b).

Geologically; the study area is mainly located in the Bahah group within the Tayyah belt (Abha quadrangle GM-75; Greewood, 1985) (Fig. 3). The Bahah group is a major component in the western part of the Tayyah belt. It consists of a fault bounded blocks including abundant volcanic greywacke, local boulder conglomerate, carbonaceous shale, slate, chert, bedded tuff, and interbeds of volcanic flow rock. In the study area there are abundant of greywacke and slate. Greywacke is characterized by massive to thin bedded in form and has sedimentary structures including grading, cross bedding, and lamina bedding. Massive greywacke forms thick beds from 1–3 m and interlayered with fine grained and laminated bedded of slate which are strongly metamorphosed to green schist facies. The Bahah group rocks in the Tayyah belt are weakly to moderately cleavage where as they are highly cleaved near faults. They are characterized by the presence of one cleavage (schistosity) which has steep dips toward east or west. Some intrusive rocks including granodiorite and granite were encountered in the Tayyah belt. Near the intrusive contact amphibolite grade metamorphic rocks were encountered. Other rock units are encountered in the surrounding areas include, alluvium and gravel, basalt and andesite, biotite monzogranite, biotite-quartzite-plagioclaae granofels, hornblende-biotite tonalite and granodiorite, Jeddah and Bahah groups, and muscovite–biotite tonalite and granodiorite.

NHESSD
3, 497–533, 2015

The area is traversed by many faults where many shear zones are located in the study area. These tectonic features are responsible for crushing and shearing of the rocks in the region. Different types of structures such as faults, folds and linear structures are encountered in the study area and its surroundings according to geological map (Abha quadrangle GM-75) (Greewood, 1985) (Fig. 3). The geological map was verified by field investigation. Along the main curvature of the study area there is a major fault that cut through the rocks (Fig. 3). The materials along the fault zone are highly crashed and weathered whereas the rocks become highly sheared and jointed as the distance increased (Greenwood, 1985).

Climatically, Saudi Arabia is classified as an arid to semi-arid region according to the "World Map of Kopper–Geiger Climate Classification" (Peel et. al., 2007). The study area is characterized by mild summers and cold winters. According to the analysis of rainfall station (A130, operated by the Ministry of Water and Electricity (MOWE) which is located in the southwest of the study area by about 20 km. Rainfall is typically occurs in intense thunderstorms from March to May. The average monthly precipitations were 29.5, 46.5, and 64 mm for March, April, and May respectively. The average annual precipitation is reported as about 273 mm yr^{-1}, with a maximum rainfall of 1043 mm occurring in 1997. The maximum precipitation happened in a day was 180 mm in 2004.

5 Results and discussion

5.1 Landslides and erosional features mapping using high resolution images

High-resolution satellite data (Quickbird image of 0.61 m resolution from the year 2012) and topographic map (scale 1 : 10 000) were used in retrieving information related to topography, existing landslides, debris accumulation and other relevant features in relation to slope instability. Satellite data was registered with reference to the topographic maps of the study area by taking input ground control points from the image and reference points from the map. The produced image was in UTM coordinate system, Zone

38, and WGS84 datum. To detect the landslides in satellite imagery, special characteristics were determined including erosion features, scares, slides, materials size, shape, tone contrast and morphological expression, and fallen materials (Fig. 4). The remote sensing findings were compared with the field photographs for the same area (Fig. 4). These features were studied along with field observation. The areas affected by landslide showed high differences in their tone than the surrounding materials as well as in some instances there are fallen materials under the landslide areas (Fig. 4). Areas have landslides typically elliptical in shape. Many potential landslide zones (rockfalls, rock sliding, circular failures, and debris channels) and erosion problems were investigated and identified in the present study as shown in Figs. 4 and 5. These landslides and erosion features along the study area were mapped on the high resolution satellite image using ArcGIS 10.2. Field checking was carried out and corrections were incorporated on the image to draw the boundary lines of the landslides. These different types of landslides and erosion features along the study area are shown in Figs. 5 and 6. In the current study, the active portions of the landslides as observed in the field and were considered for the hazard assessment. Mostly the active parts of the landslide located above the road level were considered in the current study to determine the impact of these landslides on the highway and the bridge piles.

5.2 Detailed field investigation of different types of landslides and erosional features

Existing and potential landslide areas were identified through field investigation along the upper portion of the escarpment highway of Tayyah valley. This includes determine different types of landslides, types of failure mechanism, lithological units, and structural data. The rock characteristics along the study area were classified into three zones (Fig. 5) according to the application of the rock mass classification system. In the current study, the RMR system was used in the analysis of the rock masses along the study area. The system first designed to analyze the rock conditions in tunnels but it was modified later to analyze slopes and foundations. The RMR system was applied

NHESSD
3, 497–533, 2015

on the 9 stations along the study area. Its value was computed, according to Bieniawski (1979), by adding rating values for five parameters including, (1) strength of intact rock, (2) RQD (measured or estimated), (3) spacing of discontinuities, (4) condition of discontinuities, and (5) water inflow through discontinuities (estimated in the worst possible conditions). The RMR value ranges between 0 and 100 has been calculated using VP EXPERT program developed by Ware Inc (1985–1988). Analysis results of rock mass rating RMR for all stations are shown in Table 1. The results indicate that there are three zones in the study area: (1) High foliated rocks are characterized by completely schistose and the RMR values range from 19 to 35 which is from poor to very poor rocks. The strength of these rocks are low to very low (Fig. 5, Table 1). (2) Fault zone is characterized by highly sheared rocks and mostly crashed, main debris flows are formed in this zone due to the presence of crashed materials and colluvial materials. The physical characteristics of these materials are composed of some boulders up to 0.5 m in diameter embedded in gravelly and fine sandy materials. The RMR values range from 16 to 19 which is very poor rocks (Fig. 5, Table 1). (3) Moderately jointed rocks which are characterized by semi massive rocks, sometimes low to moderately strong and characterized by the presence of planar and raveling types of failure; they are intruded by some felsic dykes. The RMR values range from 65 to 74 which is good (Fig. 5, Table 1).

Landslides in the study area were mapped, identified, and classified into rock falls (raveling failure types) and rock slides (planar failure). The planar types are predominantly along discontinuities. These raveling and sliding failures are mainly located in zone 1 and 3 (Fig. 6). In zone 2 (fault zone), debris flow, circular failure, raveling types, and sometimes complex circular failures are detected. In the complex circular failures multiple failure modes, many tension cracks, and subsidence are located along the highly sheared and colluvial materials above the bridge level. Field investigations showed that the most landslide materials in zone 2 (fault zone) are mainly composed of boulders, rock fragments and soil (Fig. 6). Debris flows are mostly confined along gullies.

NHESSD
3, 497–533, 2015

Landslides along the highway section and along the drainage systems (gullies) are occurring on the slopes that vary generally from 30 to 85°. The study area is highly affected by faults and most of the rock in the area is highly jointed and mixed together as well as many colluvium soils are located with different sizes where shallow debris overburden extending below the bridge. The loose overburden materials, when saturated during rains, form debris flows. These sliding blocks and the debris flows are affected the bridge piles. In addition the running water are causing erosion (scouring) of the areas between and around the bridge piles (Fig. 6). These different types of landslides impose threatening to the road and bridge. Other type of threatening problem that is related to the erosional effect of the running water through the drainage channels (gullies) that cut through the mountain and run under the bridge and through culverts. There are many drainage channels (gullies) that found in the study area that impose erosion impact under and between the bridge piles and under the culverts (Fig. 6). The erosional and debris flows could be a problem in the future and will pose threat to the stability of the bridge and cause damages to vehicles and disrupts traffic.

5.3 Erosion problems under and between the bridge piles

Many authors focused their studies on rill and inter-rill erosion (Poesen and Hooke, 1997). Others focused on gullies erosions and they indicated that these gullies represent the main sediment source in Mediterranean environments (Casali et al., 1999; Poesen et al., 2002, 2003; Valcarcel et al., 2003). The erosion processes in the study area have a severe effect in the areas between bridge piles and the area along the drainage channels (gullies). In the current study, detailed drainage network were drawn from the high resolution satellite image and filed investigations and were compared with the networks that extracted from SRTM 90 m and Digital elevation model of 5 m resolution (created from topographic map of 1 : 10 000) using watershed modeling system (WMS 8.1) (Fig. 7). Different types of morphometric parameters were determined for each gully to determine its activity in erosion effect (Table 2). Existing and potential erosion areas were identified through field investigation along the study area and by using high resolution image. The erosion materials can cause the debris flow to occur after the gradual increase in discharge. Width of the existing gullies ranges from 6 to 15 m whereas the depth of erosions was determined to be from 2 to 5 m (Table 2). Field investigation indicated that most of the gullies are cut through foliated rocks (zone 1) which includes channels 6, 7, 8, 9, and 10, and the fault zone (zone 2) which includes channels 2, 3, 4, and 5. However, few gullies are located in moderately jointed rocks (zone 3) which include channel 1. In the study area most of rocks here are highly foliated (metamorphic), sometimes intruded by different dykes (of acidic igneous rocks). These rocks are overlaid by loose residual soils and slope wash. After the rainfall and with continuities of debris flow, the loose soil cover (debris materials and crashed rocks along the fault plane) are moved away and bare rocks are now exposed on the side walls and at the bottom of the gullies (Figs. 5 and 6). At the surface of the rocks, and between the bridges piles there are scouring effect (erosions). These debris coming from these areas moved with water toward the main wadi course. Data analysis and field investigation indicated that there are three factors that play a major influence in the erosion processes and which are claimed to be the most important causes of channel erosion. These factors include high runoff due to intense rainfall, weak materials that is located along the gullies, and the steepening slope of these gullies (Table 2).

5.4 Evaluation of landslides types in the study area

Many landslide potential zones were identified in the study area. These zones have main impacts on the bridge piles and thereby posing threat to lives and properties. Landslides identified in the study area are broadly classified into rock slide, circular failure, and debris flows which represent the most threatening landslides in this area. Some of these landslides are shown in Fig. 6.

NHESSD
3, 497–533, 2015

5.4.1 Planner failures

In general, most slope failures, that are structurally controlled, can be classified into one of four categories depending on the geometrical and mechanical nature of the discontinuities and rock mass conditions. These slope failures include circular, planner, wedge, and toppling failures. In many areas the discontinuities are oriented in such a way that they contribute to these types of failures. In the curent study three locations were examined. These sites impose planner failures from time to time. In the current study the Bahah group has weakly to moderately cleavage and highly cleaved near fault zone. Sometimes they are characterized by the presence of one cleavage (schistosity) which has steep dips toward the bridge section as in site 3. Some intrusive and volcanic dykes were encountered in the Tayyah belt. These gives large planner failures where the joints dips towards the road bridge section as shown in sites 1 and 2. Data collected from these sites were plotted on stereonets (Fig. 8). Sites 1 and 2 are located in moderately jointed zone and their main joint sets are characterized by a dip directions ranges from 7 to 17° and dip angle from 48 to 59° (Table 3, Fig. 9). Field investigations, for these two sites indicate that both are examined large planner failures. By comparing the strike of the bridge section and these two locations indicated that they are nearly parralled. In addition, the site 3 is located in higly foliated rocks that showing a shestosity texture and the main joint set has a dip directio of 5° and dip angle of 80° which is parallel to strike of the bridge section. The dip/dip direction measurements that collected from these three sites were plotted on stereonets using Dips 5 software (RocScience, 1999). The dip is defined as the maximum inclination of a structural discontinuity plane measured from the horizontal. The dip direction is the direction of the horizontal trace of the line of dip measured clockwise from north (ISRM, 1981). Stereographic analysis allows investigators to visualize and measure discontinuities in three-dimensions by projection discontinuity planes through a sphere and observing the trace of the line of intersection of the plane and sphere (Fig. 9). A structural control stability analysis utilizing the Markland Test Plot method, was used to assess the potential for planner sliding along the identified discontinuities. Markland test plots show the discontinuities in relation to potential planner sliding surfaces on a lower hemisphere stereonet projection. The slope face is shown as a marked great circle and the measured friction angle is represented by an interior circle. Based on discontinuity roughness and other properties of the rock, friction angles in this study have been meaured using different techniques including (1) rock data analysis of the field rock mass characteristics; and, (2) rock shear box for the samples along the critical joints in these sites. The lowest friction angle and dip direction of the joints and rock cut were used to determine the potential planner failure. If discontinuity dip vectors plot within the shaded areas of the test plot, failure along the discontinuity is kinematically possible. Table 3 shows the different characteristics of each site and Fig. 9 shows the stereonet presentations of the main discontinuity data collected from the rock cut stations above the bridge section of the study area. In the current study lowest measured friction angle of 35, 40, and 30° was used for these three sites respectively (based on the shear strength and rockdatat analysis) (Table 3). The dip vectors of these three main joints sets occur within the crescent shaped shaded area, in addition the strike of these main joints have an angle less than 20° from the strike of the rock cut face and so planar failure for these main joints are potential.

5.4.2 Circular failures

Circular failures sometimes occur in intensely fractured rock masses in relation to the scale of the slope that they may be considered as randomly jointed and isotropic. In highly weathered materials, non-circular failures may occur along a combination of existing joints and failure through weak but previously intact material. In circular failures, there is no structural pattern and the failure surface is free to find the line of least resistance through the slope and the failure geometry is circular (Hoek and Bray, 1981). This is the most common type of low slope failure in soil or in material such as mine waste in which no regular pattern of geologic features exist (Hoek, 1982). Landslide materials, especially along the fault zone, are mainly composed of boulders, rock fragments and

NHESSD
3, 497–533, 2015

soil (sandy materials). Many circular failures were detected in the study area and some of them are clearely appeared in Fig. 6c. Whereas other circular failures are new where some tension cracks begin to be appeared at the upper portion of the bench located above the bridge level (Fig. 10a–c).

5.4.3 Raveling failures

This type of failure that occure due to a combination of different factors and not related to the structures (joint planes). In most of the rock cuts and slopes, rockfalls are difficult to analyze. Badger and Lowell (1992) mentioned that large number of accidents and about half dozen fatalities were related to rockfalls (ravelling failures) in the last 30 years. In the study area, most of ravelling failures (rockfalls) are related to the effect of undercutting of the week materials or due to sliding effect and leave other blocks hanging over (Fig. 10d and e), others related to erosional effect of rainfall especially in debris and colluvium materials where the weake materials eroded and leaving large blocks without any support (Fig. 10f). With the effect of gravety, rainfall, and vibration due to heavy trucks, these overhaning materials will fall down.

5.4.4 Debris flows

In the study area, the debris flows are mostly confined along natural drainage lines as well as along the fault zone. Debris flows are occurring along the gullies with an average slopes that vary from 13.2° for channel 1 to 32.2° for channel 7 (Figs. 5 and 7). Most of the debris flows occur along the gullies where loose overburden materials on such slopes, when saturated during rains causes debris flows. This happened very often and these debris flows have an erosion effect along the gullies and between the bridge piles. Where most of weak materials, highly jointed rocks, and colluvial soils erode and moved downwards with running water. The debris flows from these gullies extend below the road and bridge level to the main wadi. Figure 6a, d, e, and f show

NHESSD
3, 497–533, 2015

some examples of debris flow channels and erosion features along the gullies in the study area.

5.5 Landslide and erosion map

Many authors such as Petley (2008) and Van Westen et al. (2006) used different data sources such as field data collection, topographical and geological maps, and satellite images interpretation to prepare landslides map. In the current study, the different types of landslides and erosion features were detected and mapped from different data sources including topographic map (1 : 10 000 scale), SRTM 90 m resolution, Landsat image (ETM$^+$ 15 m), QuickBird image (0.6 m) and extensive field investigation (Fig. 2). These data were collected and assembled together using Arc GIS 10.2 to create a landslide and erosion map of the study area (Fig. 11). This final map shows the distribution of different types of landslides and erosion features problems in the study area including locations of debris flows, rockfalls, translational sliding, few rotational failures and erosional features along different gullies.

6 Mitigation strategies

From engineering point of view there are various types of measures that can be used to reduce the impact of landslides on the highway (bridge section) section between tunnel 7 and tunnel 8. An outline of different mitigation methods for debris flows and landslides as potential methods were given by different authors (deWolfe, 2006; deWolfe et al., 2008; Franzi et al., 2011; Huebl and Fiebiger, 2005; Maerz et al., 2014; Wagenbrenner et al., 2006; You et al., 2012; Youssef et al., 2012, 2014b).

In the current study different mitigation and remediation techniques could be used from future landslides and erosional flows. The generation of debris flow, runoff erosion, sliding failures, and raveling processes acting on the entire study area were taken into account. For the current study, the slides, raveling, debris flows and running water

NHESSD
3, 497–533, 2015

cause different type of problems. The effectiveness of landslide and erosion control treatments in the study area has been evaluated. Thus the aim of mitigation is to prevent different types of landslides and running water effect (erosion problems between bride piles), which includes reducing the velocity of water flow, preventing down cutting erosion and decreasing the gradient of the gully. The mitigation methods proposed in the current study include:

(1) Controlling the landslides by applying a suitable remediation/mitigation technique. Slope stabilization has to be done for the rock cuts and slopes above the bridge and highway level, this will reduce the volume of the initial material. For the unstable faces, shotcrete (the sprayed concrete process) have to be applied. Drainage ditches has to be established above the potential failures to divert the water and prevent infiltration into potential unstable areas, and benches have to be cleaned and established below the potential failures to increase the space to accommodate the falling rocks.

(2) for the gullies with the effect of debris flows and erosion features, land management techniques have to be applied to decrease the erosional features by runoff diversion from the gullies at different levels along the benches. In the areas surrounding the bridge piles and under the culverts from up and down streams sides a layer of shotcrete need to be established in order to protect the area from scouring effect and protect the piles and culvert from any damage. In addition along the gullies grid dams need to be installed to reduce the velocity of water flow by decreasing the gradient of the gully and to stabilize slopes. This will provide barriers against runoff to reduce the erosion and resulting in a reduction for erosion potential.

7 Conclusions

In the upper portion of Tayyah valley in Asir region, Saudi Arabia, there are many active landslides and erosion features particularly along the escarpment road especially between tunnels 7 and 8, which are not only threatening human lives, but also causing damages to highway and bridge foundation. A detailed study along the upper portion of

NHESSD
3, 497–533, 2015

Al-Tayyah escarpment highway between tunnel 7 and tunnel 8 showed that this highway section (bridge) has been subjected to repeated landslide activities, and erosional effect due to runoff and debris flows along the gullies that dissect the study area as a result this section of the highway is under severe risk. Rainfall in the study area can cause different types of landslides such as debris flows along the existing gullies that will increase the erosion effect along these gullies. These debris flows and erosion effect will impact the areas under and between the bridge piles and under the culverts making undercutting features.

In addition, it was observed that the highway section (bridge) between tunnel 7 and tunnel 8 are prone to different types of landslides and erosion features. These landslides include debris flows, planar sliding, circular failures, and raveling failure types. The study area was classified into three zones, according to the geological engineering characteristics of these zones. Zone 1 is characterized by high foliated rocks (Schistose rocks) and it is dominated by planar and raveling type of failures; zone 2 (fault zone area) is characterized by sheared and crashed rocks and this zone is dominated by circular type of failure; and zone 3 is characterized by moderately jointed rocks and this zone is dominated by planar and raveling types of failures. Debris flows and erosion features along the gullies are distributed in all zones and it is more effective and high dense in zone 2 due it its lithological and structural characteristics where most of this zone is sheared and crushed materials due to the fault. Different types of mitigation techniques have been proposed to protect, minimize, and/or prevent the impact of these landslides and runoff erosional features of the gullies on the study area.

References

Alimohammadlou, Y., Najafi, A., and Gokceoglu, C.: Estimation of rainfall-induced landslides using ANN and fuzzy clustering methods: a case study in Saeen Slope, Azerbaijan province, Iran, Catena, 120, 149–162, 2014.

Badger, T. C. and Lowell, S.: Rockfall control Washington State, in: Rockfall Prediction and Control and Landslide Case Histories, Transportation Research Record, National Research Council, Washington, 1342, 14–19, 1992.
Baum, R. L. and Godt, J. W.: Early warning of rainfall-induced shallow landslides and debris flows in the USA, Landslides, 7, 259–272, doi:10.1007/s10346-010-0204-1, 2010.
Carrara, A., Cardinali, M., Guzzetti, F., and Reichenbach, P.: GIS technology in mapping landslide hazard, in: Geographical Information Systems in Assessing Natutral Hazards, edited by: Carrara A. and Guzetti F., Kluwer Academic Publishers, the Netherlands, 135–176, 1995.
Casali, J., Lopez, J. J., and Giraldez, J. V.: Ephemeral gully erosion in southern Navarra (Spain), Catena, 36, 65–84, 1999.
Chung, C. F. and Fabbri, A. G.: Probabilistic prediction models for landslide hazard mapping, Photogramm. Eng. Rem. S., 65, 1389–1399, 1999.
De La Ville, N., Diaz, A. C., and Ramirez, D.: Remote sensing and GIS technologies as tools to support sustainable management of areas devastated by landslides, Environment, development and sustainability, 4, 221–229, 2002.
deWolfe, V.: An evaluation of erosion control methods after wildfire in debris-flow prone areas, M.S. thesis, Colorado School of Mines, Golden, CO, 185 pp., 2006.
deWolfe, V., Santi, P., Ey, J., and Gartner, J.: Effective debris flow mitigation at Lemon Dam, LaPlata County, Colorado, Geomorphology, 96, 366–377, 2008.
Dhakal, A. S., Amada, T., and Aniya, M.: Landslide hazard mapping and its evaluation using GIS: an investigation of sampling schemes for a grid-cell based quantitative method, Photogramm. Eng. Rem. S., 66, 981–989, 2000.
Farrokhnia, A., Pirasteh, S., Pradhan, B., Pourkerman, M., and Arian, M.: A recent scenario of mass wasting and its impact on the transportation in Alborz Mountains, Iran: contribution from Geo information technology, Arab. J. Geosci., 4, 1337–1349, 2010.
Fell, R., Corominas, J., Bonnard, C., Cascini, L., Leroi, E., and Savage, W.: Guidelines for landslide susceptibility, hazard and risk zoning for land use planning, Eng. Geol., 102, 85–98, 2008.
Franklin, J. A. and Senior, S. A.: Rockfall hazards – strategies for detection, assessment, and remediation, Paper presented at: Proceedings International Symposium on Engineering Geology and the Environment, Athens, Greece, 657–663, 1997.
Franzi, L., Giordan, D., Arattano, M., Allasia, P., and Arai, M.: Preface Results of the open session on “Documentation and monitoring of landslides and debris flows” for mathematical

NHESSD
3, 497–533, 2015

modelling and design of mitigation measures, held at the EGU General Assembly 2009, Nat. Hazards Earth Syst. Sci., 11, 1583–1588, doi:10.5194/nhess-11-1583-2011, 2011.
Frenez, T., Roth, A., and Kaestli, A.: Debris flow mitigation by means of flexible barriers, Pare presented at: Proceedings of the 10th Congress Interpraevent 2004, Trento, Italy, 2004.
Greenwood, W. R.: Geologic map of the Abha quadrangle, sheet 18 F, Kingdom of Saudi Arabia, Ministry of Petroleum and Mineral Resources, Deputy Ministry for Mineral Resources GM-75 c, scale 1 : 250,000, 1985.
Guzzetti, F., Carrara, A., Cardinali, M., and Reichenbach, P.: Landslide hazard evaluation: an aid to a sustainable development, Geomorphology, 31, 181–216, 1999.
Guzzetti, F., Peruccacci, S., Rossi, M., and Stark, C. P.: The rainfall intensity duration control of shallow landslides and debris flows: an update, Landslides, 5, 3–17, 2008.
Hoek, E.: Recent rock slope stability research at the Royal School of Mines, London, in: Geotechnical Practice for Stability in Open Pit Mining, edited by: Brawner, C. O. and Milligin, V., the American Institute of Mining, Metallurgical, and Petroleum Engineers, Inc., New York, 27 pp., 1982.
Hoek, E. and Bray, J. W.: Rock Slope Engineering, In-stitution of Mining and Metallurgy, Spon Press, London, p. 368, 1981.
Huebl, J. and Fiebiger, G.: Debris flow mitigation measures, in: Debris-flow Hazards and Related Phenomena, edited by: Jakob, M. and Hungr, O., Springer Verlag, Berlin, 445–488, 2005.
Hungr, O., Morgan, G. C., VanDine, D. F., and Lister, D. R.: Debris flow defences in British Columbia. in: Debris Flows/Avalanches: Process, Recognition and Mitigation, Reviews in Engineering Geology, edited by: Costa, E., Wieczorek, G. F., Geol. Soc. Am., Boulder, Colorado, 201–222, 1987.
Hungr, O., Evans, S. G., Bovis, M. J., and Hutchinson, J. N.: A review of the classification of landslides in the flow type, Environ. Eng. Geosci., 7, 221–228, 2001.
International Society for Rock Mechanics (ISRM): Rock characterization, testing and monitoring. in: ISRM Suggested Methods, edited by: Brown, E. T., Pergamon Press, Oxford, UK, 211 pp., 1981.
Iverson, R. M., Reid, M. E., Logan, M., LaHusen, R. G., Godt, J. W., and Griswold, J. P.: Positive feedback and momentum growth during debris-flow entrainment of wet bed sediment, Nat. Geosci., 4, 116–121, 2011.

NHESSD
3, 497–533, 2015

Johnson, A. M.: Debris flow, in: Slope Instability, edited by: Brunsden, D. and Prior, D. B., Wiley, New York, 257–361, 1984.

Lan, H. X., Zhou, C. H., Wang, L. J., Zhang, H. Y., and Li, R. H.: Landslide hazard spatial analysis and prediction using GIS in the Xiaojiang watershed, Yunnan, China, Eng. Geol., 76, 109–128, 2004.

Maerz, N. H., Youssef, A. M., Pradhan, B., and Bulkhi, A.: Remediation and mitigation strategies for rock fall hazards along the highways of Fayfa Mountain, Jazan Region, Kingdom of Saudi Arabia, Arab. J. Geosci., doi:10.1007/s12517-014-1423-x, online first, 2014.

Peel, M. C., Finlayson, B. L., and McMahon, T. A.: Updated world map of the Köppen-Geiger climate classification, Hydrol. Earth Syst. Sci., 11, 1633–1644, doi:10.5194/hess-11-1633-2007, 2007.

Petley, D. N.: The global occurrence of fatal landslides in 2007, Geophysical Research Abstracts, Vol. 10, EGU General Assembly 2008, EGU2008-A-10487, 3 pp., 2008.

Pierson, T. C. and Costa, J. E.: A rheologic classification of subaerial sediment-water flows, in: Debris Flows/Avalanches: Process, Recognition and Mitigation, Reviews in Engineering. Geology, edited by: Costa, J. E. and Wieczorek, G. F., Geol. Soc. Am., Boulder, Colorado, 1–12, 1987.

Poesen, J., Vandekerckhove, L., Nachtergaele, J., Oostwoud Wijdenes, D., Verstraeten, G., and Van Wesemael, B.: Gully erosion in dry land environments, in: Dry Land Rivers: Hydrology and Geomorphology of Semi-Arid Channels, edited by: Bull, L. J. and Kirkby, M. J., Wiley, Chichester, England, 229–262, 2002.

Poesen, J., Nachtergael, J., Verstraeten, G., and Valentin, C.: Gully erosion and Environmental change: importance and research needs, Catena, 50, 91–133, 2003.

Poesen, J. W. A. and Hooke, J. M.: Erosion, flooding and channel management in the Mediterranean environments of southern Europe, Prog. Phys. Geog., 21, 157–199, 1997.

Pourghasemi, H. R., Mohammadi, M., and Pradhan, B.: Landslide susceptibility mapping using index of entropy and conditional probability models at Safarood Basin, Iran, Catena, 97, 71–84, doi:10.1016/j.catena.2012.05.005, 2012.

Prochaska, A. B., Santi, P. M., Higgins, J. D., and Cannon, S. H.: A study of methods to estimate debris flow velocity, Landslides, 5, 431–444, 2008.

Regmi, A. D., Yoshida, K., Dhital, M. R., and Devkota, K.: Effect of rock weathering, clay mineralogy, and geological structures in the formation of large landslide, a case study from

Dumre Besei landslide, Lesser Himalaya Nepal, Landslides, 10, 1–13, doi:10.1007/s10346-011-0311-7, 2013a.
Regmi, A. D., Devkota, K. C., Yoshida, K., Pradhan, B., Pourgasemi, H. R., K umamoto, T., and Akgun, K.: Application of frequency ratio, statistical index, and weights-of evidence models and their comparison in landslide susceptibility mapping in Central Nepal Himalaya, Arab. J. Geosci., 7, 725–742, doi:10.1007/s12517-012-0807-z, 2013b.
Regmi, A. D., Yoshida, K., Nagata, H., and Pradhan. B.: Rock toppling assessment at Mugling–Narayanghat road section: "A case study from Mauri Khola landslide", Nepal, Catena, 114, 67–77, doi:10.1016/j.catena.2013.10.013, 2014.
Rickenmann, D.: Empirical relationships for debris flows, Nat. Hazards, 19, 47–77, 1999.
Rimbock, A. and Strobl, T.: Loads on rope net constructions for woody debris entrapment in torrents, International Congress "Interpraevent in the Pacific Rim", Matsumoto, Japan, Congress publication, 2, 797–807, 2002.
Rocscience, Ltd.: DPS 5.0 software for graphical and statistical analysis of orientation based geological data, Toronto, Ontario, available at: www.rocscience.com (last access: 23 July 2011), 1999.
Shahabi, H., Khezri, S., Bin Ahmad, B., and Hashim, M.: Landslide susceptibility mapping at central Zab basin, Iran: a comparison between analytical hierarchy process, frequency ratio and logistic regression models, Catena, 115, 55–70, 2014.
Shroder, J. F. and Bishop, M. P.: Mass movement in the Himalaya: new insights and research directions, Geomorphology, 26, 13–35, 1998.
Tien Bui, D., Pradhan, B., Lofman, O., Revhaug, I., and Dick, O. B.: Spatial prediction of landslide hazards in Hoa Binh province (Vietnam): a comparative assessment of the efficacy of evidential belief functions and fuzzy logic models, Catena, 96, 28–40, 2012.
Umar, Z., Pradhan, B., Ahmad, A., Jebur, M. N., and Tehrany, M. S.: Earthquake induced landslide susceptibility mapping using an integrated ensemble frequency ratio and logistic regression models in West Sumatera Province, Indonesia, Catena, 118, 124–135, 2014.
Valcárcel, M., Taboada, M. T., and Dafonte, J.: Ephemeral gully erosion in northwestern Spain, Catena, 50, 199–216. 2003.
Van Westen, C. J.: GIS in landslide hazard zonation: a review, with examples from the Andes of Colombia, in: Mountain Environments and Geographic Information System, edited by: Price, M. and Heywood, I., Taylor & Francis, Basingstoke, 135–165, 1994.

NHESSD
3, 497–533, 2015

Van Westen, C. J., Van Asch, T. W. J., and Soeters, R.: Landslide hazard and risk zonation – why is it still so difficult?, B. Eng. Geol. Environ., 65, 167–184, 2006.

Wagenbrenner, J., Macdonald, L., and Rough, D.: Effectiveness of three post-fire rehabilitation treatments in the Colorado Front Range, Hydrol. Process., 20, 2989–3006, 2006.

You, Y., Liu, J. F., Pan, H. L., and Chen, X. Z.: Debris flow hazards and the optimal characteristics of the drainage canal for Zhangjia gully, Beichuan county following the 5.12 Wenchuan earthquake, Environ. Earth Sci., 65, 1005–1012, 2012.

Youssef, A. M., Maerz, N. H., and Hassan, A. M.: Remote sensing applications to geological problems in Egypt: case study, slope instability investigation, Sharm El-Sheikh/Ras-Nasrani Area, Southern Sinai, Landslides, 6, 353–360, doi:10.1007/s10346-009-0158-3, 2009.

Youssef, A. M., Maerz, H. N., and Al-Otaibi, A. A.: Stability of rock slopes along Raidah escarpment road, Asir Area, Kingdom of Saudi Arabia, J. Geogr. Geol., 4, 48–70, doi:10.5539/jgg.v4n2p48, 2012.

Youssef, A. M., Pradhan, B., and Maerz, N. H.: Debris flow impact assessment caused by 14 April 2012 rainfall along the Al-Hada Highway, Kingdom of Saudi Arabia using high-resolution satellite imagery, Arab. J. Geosci., 7, 2591–2601, doi:10.1007/s12517-013-0935-0, 2013.

Youssef, A. M., Al-kathery, M., and Pradhan, B.: Landslide susceptibility mapping at Al-Hasher Area, Jizan (Saudi Arabia) using GIS-based frequency ratio and index of entropy models, Geosci. J., doi:10.1007/s12303-014-0032-8, online first, 2014a.

Youssef, A. M., Al-kathery, M., Pradhan, B., and Elsahly, T.: Debris flow impact assessment along the Al-Raith Road, Kingdom of Saudi Arabia, using remote sensing data and field investigations, Geomatics, Natural Hazards and Risk, doi:10.1080/19475705.2014.933130, online first, 2014b.

NHESSD

3, 497–533, 2015

Assessment of impact of mass movements on the upper Tayyah valley's bridge

A. M. Youssef et al.

Title Page
Abstract | Introduction
Conclusions | References
Tables | Figures
◂◂ | ▸▸
◂ | ▸
Back | Close
Full Screen / Esc
Printer-friendly Version
Interactive Discussion

Table 1. RMR values for different stations along the study area.

Zone #	Station #	UCS MPa	RQD	Spacing of discontinuities	Condition of discontinuities	Water general condition	RMR basic	Rock Class
Z1	1	1–5	< 25	< 60 mm	Soft gouge > 5 mm thick Or Separation > 5 mm Continuous	Damp	19	Very poor rocks
	2	3–25	25–50	60–200 m	Slickensided surfaces Or Gouge < 5 mm thick Or Separation 1–5 mm	Wet	35	Poor rocks
	3	3–25	< 25	< 60 mm	Slickensided surfaces Or Gouge < 5 mm thick Or Separation 1–5 mm	Damp	30	Poor rocks
Z 2	4	1–5	< 25	< 60 mm	Soft gouge > 5 mm thick Or Separation > 5 mm Continuous	Damp	19	Very poor rocks
	5	1–5	< 25	< 60 mm	Soft gouge > 5 mm thick Or Separation > 5 mm Continuous	Wet	16	Very poor rocks
	6	1–5	< 25	< 60 mm	Soft gouge > 5 mm thick Or Separation > 5 mm Continuous	Wet	16	Very poor rocks
	7	1–5	< 25	< 60 mm	Soft gouge > 5 mm thick Or Separation > 5 mm Continuous	Damp	19	Very poor rocks
Z3	8	50–100	50–75	0.6–2 m	Slightly rough surfaces Separation < 1 mm. Highly weathered walls	Damp	65	Good
	9	100–250	50–75	0.6–2 m	Slightly rough surfaces Separation < 1 mm. Highly weathered walls	Damp	70	Good
	10	100–250	75–90	< 60 mm	Slightly rough surfaces Separation < 1 mm. Highly weathered walls	Damp	74	Good

NHESSD
3, 497–533, 2015

Table 2. General characteristics of the gullies and different rock zones.

	Ch_01	Ch_02	Ch_03	Ch_04	Ch_05	Ch_06	Ch_07	Ch_08	Ch_09	Ch_10
H_Max	2163	2153	2145	2139	2136	2035	2127	2149	2113	2111
H_Min	1920	1964	1925	1835	1844	1843	1707	1793	1842	1877
Hmax-Hmin	243	189	220	304	292	192	420	356	271	234
Length	826	526	319	783	588	360	587	831	598	538
Tan (θ)	0.294	0.359	0.690	0.388	0.497	0.533	0.716	0.428	0.453	0.435
Slope Degree (θ)	13.2°	16.2°	31.0°	17.5°	22.4°	24.0°	32.2°	19.3°	20.4°	19.6°
Width (m)	15	11	9	8	7	10	8	8	6	8
Depth of erosion (m)	Up to 2 m	Up to 5 m				Up to 3 m				
Zone Name	Moderate jointed rocks	Fault zone				High foliated rocks				
Main characteristics	Planar failures and raveling	Circular failures and debris flows				Planar failure				

NHESSD
3, 497–533, 2015

Table 3. Shows different characteristics of each site.

Site Number	Main Joints		Rock Cut face		Friction angle (⌀)
	Dip angle	Dip direction	Dip angle	Dip direction	
1	48°	17°	80°	12°	35
2	59°	7°	80°	2°	40
3	80°	5°	85°	13°	30

D = Dip; DD = Dip Direction, =Friction Angle.

NHESSD
3, 497–533, 2015

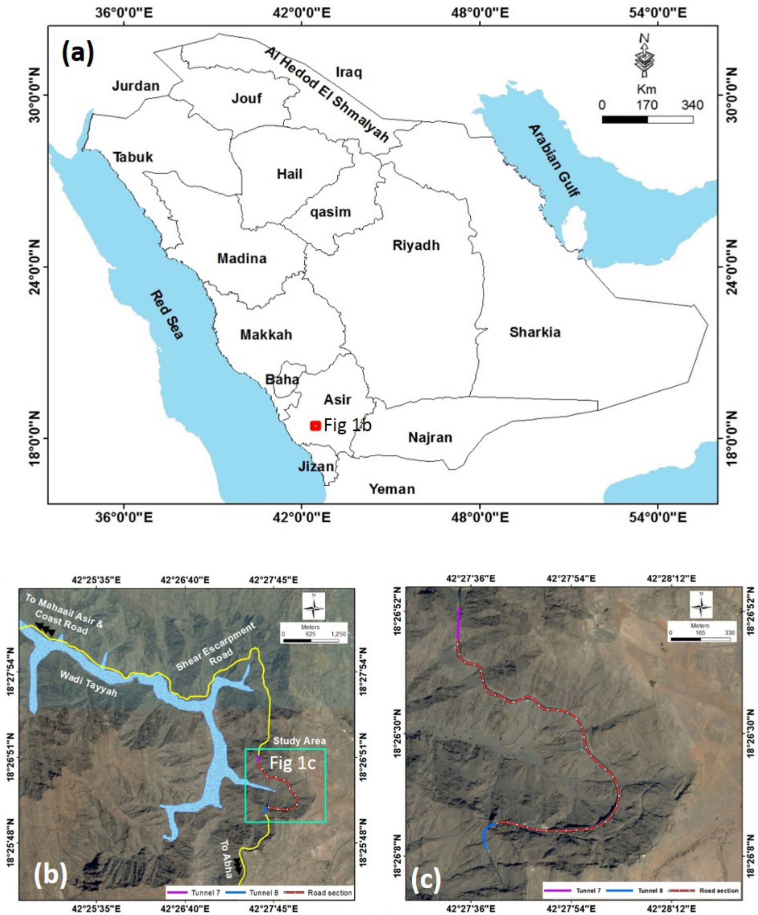

Figure 1. (a) Location of the study area in the KSA map. **(b)** Upper portion of Tayyah Valley including the study area. **(c)** Study area in a close up view.

NHESSD

3, 497–533, 2015

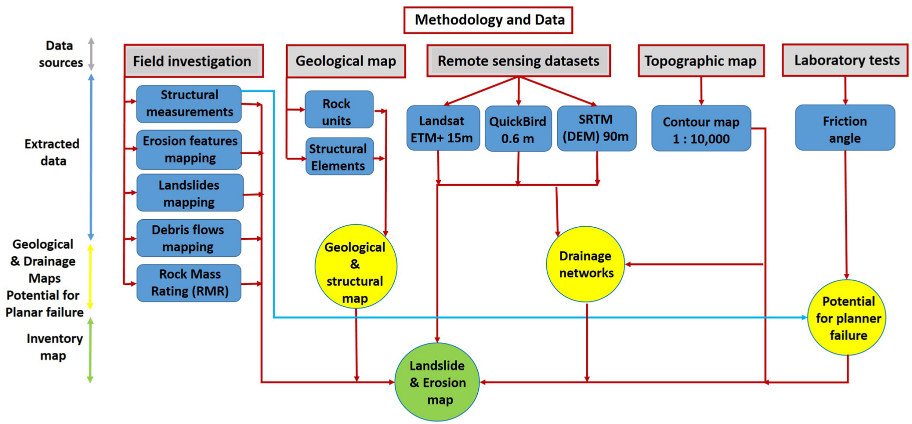

Figure 2. Flow chart showing data used and methodology in the study area.

NHESSD
3, 497–533, 2015

Assessment of impact of mass movements on the upper Tayyah valley's bridge

A. M. Youssef et al.

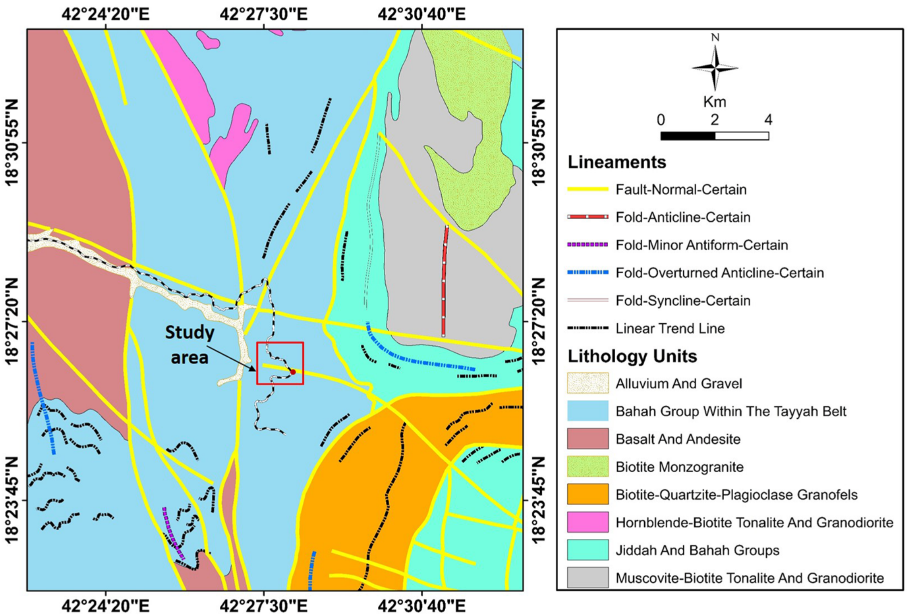

Figure 3. Geological map of the study area and its surroundings at the upper portion of the Tayyah Valley.

NHESSD
3, 497–533, 2015

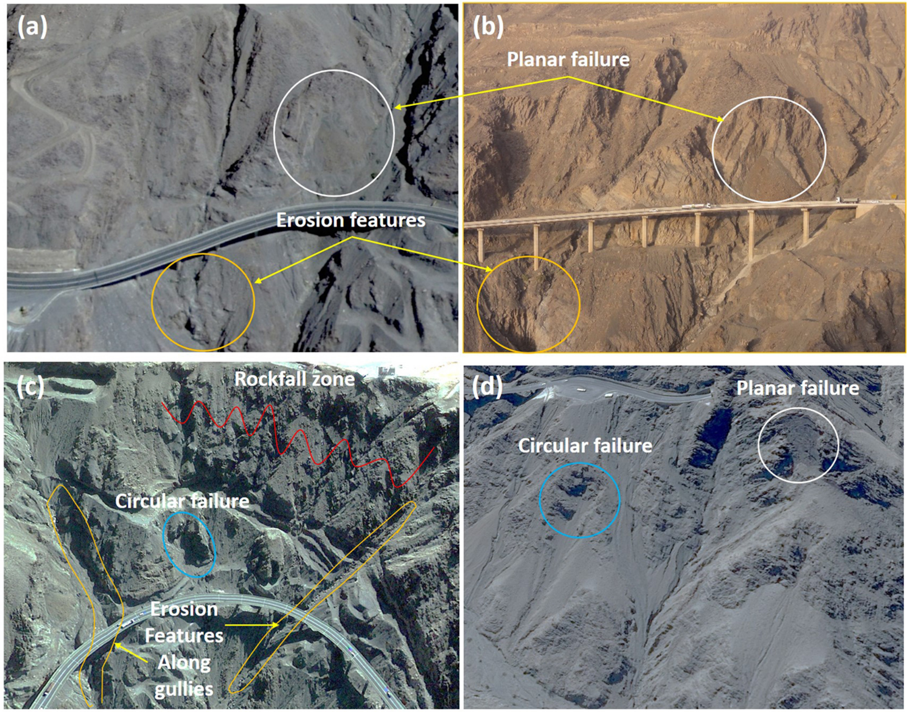

Figure 4. (a) Different landslides features can be detected using high resolution satellite image; **(b)** same landslides features appeared in field photograph in the same area; (**c** and **d**) planar, circular, rockfall zone and erosion features as they appear in high resolution satellite image (3-D images).

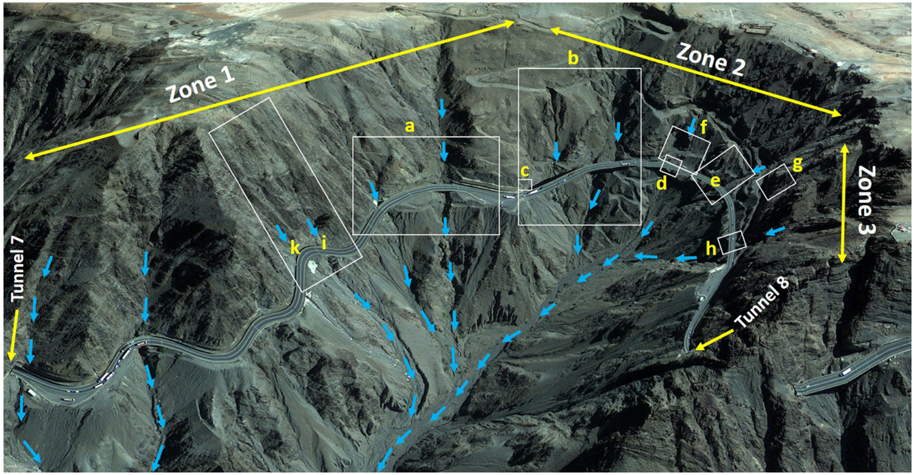

Figure 5. 3-D view showing the potential gullies causing debris movements and erosions under and between the bridge piles as well as the areas for different types of landslides. 3-D image was prepared using QuickBird imagery. Note, the study area between tunnels 7 and 8 shows three zones and different landslides locations can be easily recognized, letters a to k are pictures in Figs. 6 and 7.

Figure 6. Field photographs showing different types of landslides and erosional features along the road section of the study area. **(a)** Sliding and erosional features due to running water along gullies, **(b)** sliding blocks along sliding plane (there are big blocks close to the bridge pile), **(c)** circular failure very close to the bridge, **(d)** deep scour features between bridge piles due to running water, **(e)** debris channels along them erosional features and big boulders appear, **(f)** debris materials of different sizes range from sand size up to big boulders 0.5 m in diameter, **(g)** large planar sliding, **(h)** deep erosion and remove the materials surround one bridge pile, (**i** and **k**) running water remove materials under the culvert make them under risk.

NHESSD
3, 497–533, 2015

A. M. Youssef et al.

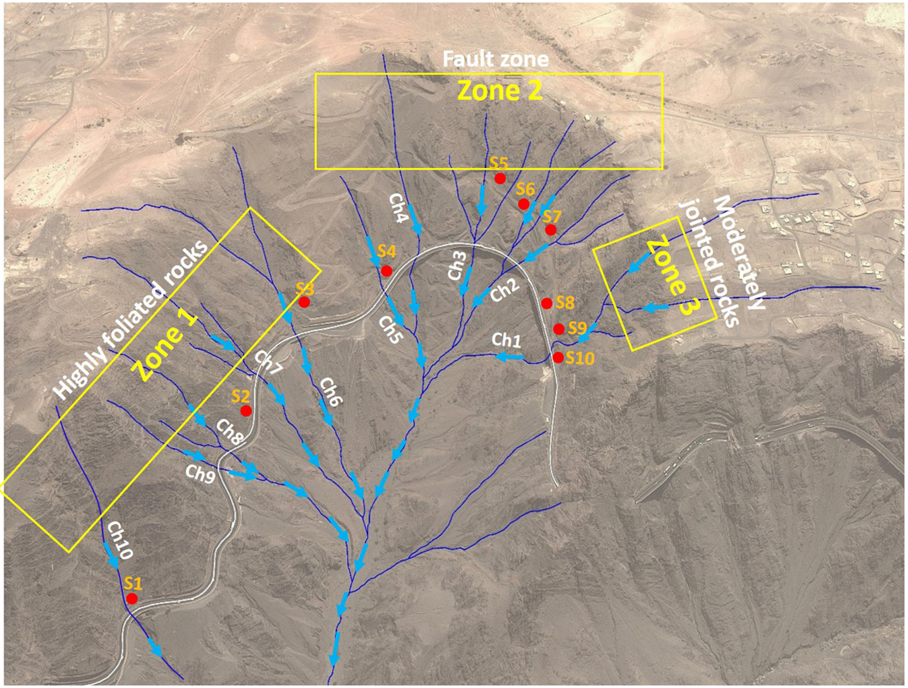

Figure 7. Different gullies were mapped in the study area as well as the stations for RMR calculation is shown as red color dots.

NHESSD
3, 497–533, 2015

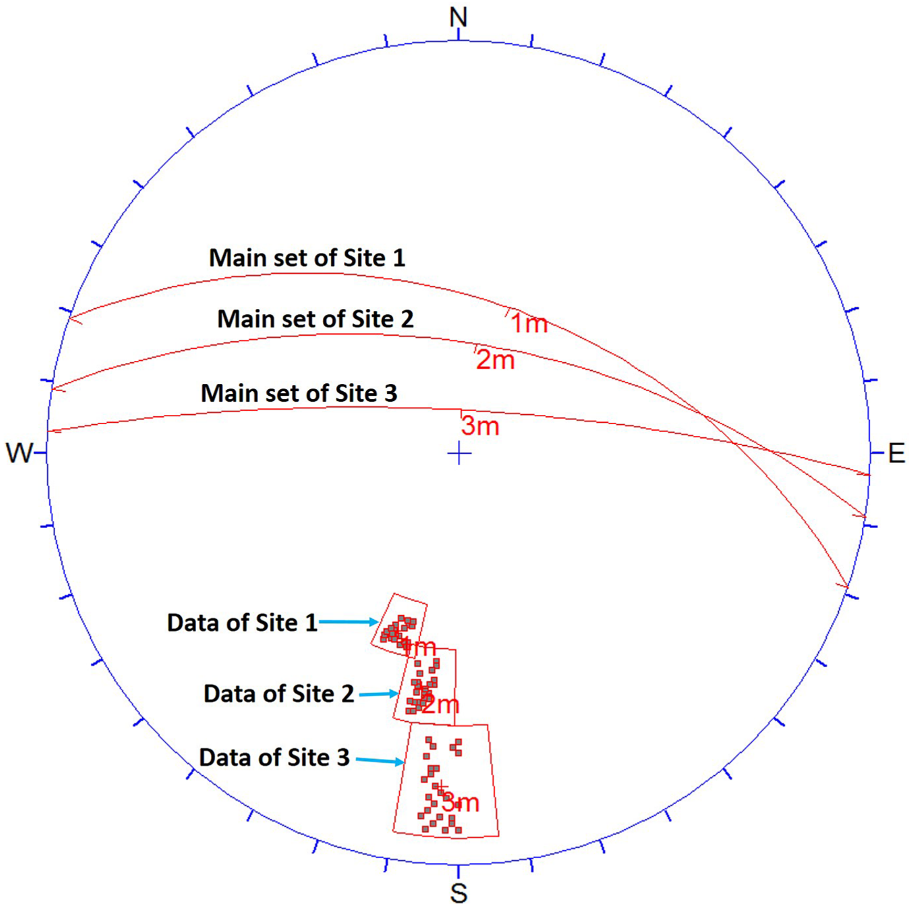

Figure 8. Pole Plots for the data collected from the three sites.

NHESSD
3, 497–533, 2015

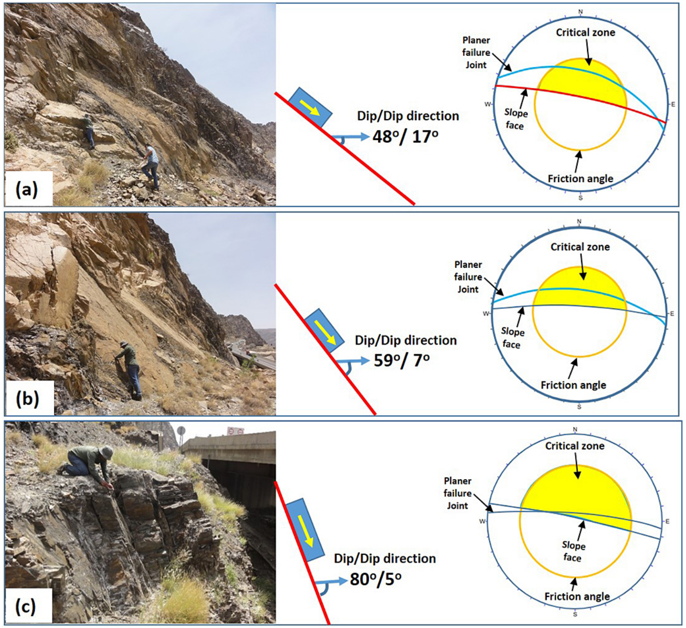

Figure 9. The analysis used in the study for planar failures along the road section of the study area: **(a–c)** Field photographs at the three locations 1, 2, 3 respectively showing the planar joints dips toward the road section, simple sketch showing the dip/dip direction average values of plane that responsible of plannar failure for each site, and Markland Test circles showing the main set, friction angle, and rock cut face for each location plotted in Dips 5 program (note that there is potential planar failures as the plot vector of planes are located in the critical zone).

NHESSD
3, 497–533, 2015

Title Page
Abstract | Introduction
Conclusions | References
Tables | Figures
◀I | ▶I
◀ | ▶
Back | Close
Full Screen / Esc
Printer-friendly Version
Interactive Discussion

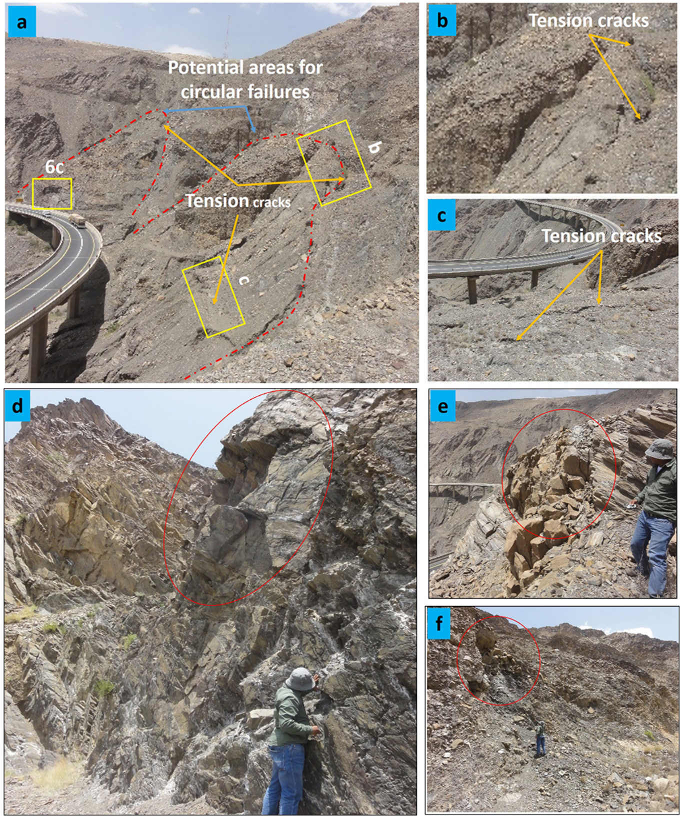

Figure 10. (a) Potentially circular failure area where some circulare failure happened and many curved tension cracks appeared, (**b** and **c**) examples of curved tension cracked. (**d** and **e**) Potentially rockfall failure area where some overhanging blocks appeared, **(f)** erosion features in debris soils causing overhanging and large blocks are prone to rockfall.

NHESSD
3, 497–533, 2015

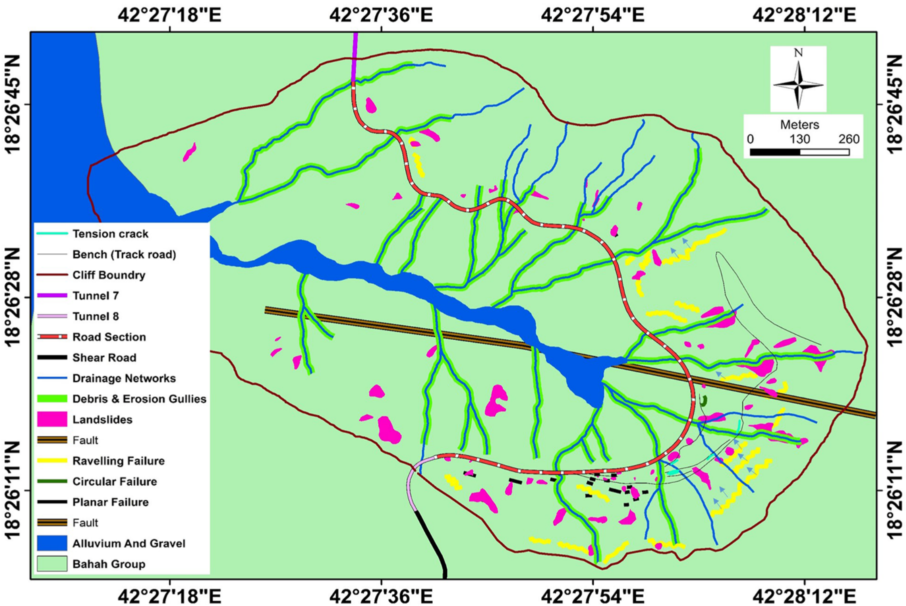

Figure 11. Inventory map of the study area showing different types of landslides, potential areas for rockfalls, planar failures, debris channels, circular failures, tension cracks and erosional features along the gullies that dissect the study area.

NHESSD
3, 497–533, 2015